RAPID COMMUNICATIONS

PHYSICAL REVIEW B VOLUME 36, NUMBER 11 15 OCTOBER 1987-I

# Lattice-dynamical analysis of the anomalous mode of W(001)

A. D. Kulkarni, F. W. de Wette, and J. Prade*
*Department of Physics, University of Texas, Austin, Texas 78712*
(Received 18 May 1987)

We construct dynamical models of W(001) by least-squares fitting the surface modes of a W(001) slab to the surface-phonon data (along $\bar{\Gamma}\bar{M}$) of Ernst *et al.* We find that the measured phonon dispersions can be explained on the basis of changes in the short-range force constants at the surface. The calculated dispersion curves along $\bar{\Gamma}\bar{X}$ depend on longer-range interactions. Thus, surface-phonon measurements along $\bar{\Gamma}\bar{X}$ may reveal whether these interactions are significant at the W(001) surface.

The (001) surface of tungsten is of great interest, experimentally as well as theoretically.[1-15] In spite of extensive investigations, it still remains a subject of several controversies. For instance, there is no agreement on the structure of this surface at high temperatures. It is believed to be disordered,[2] or ordered and $p(1\times1)$.[3,4] At low temperatures it undergoes a $(\sqrt{2}\times\sqrt{2})R45°$ reconstruction.[5-7] But the significance of the long-range interactions for this surface, especially in its reconstruction, remains controversial.[8-10] So far these studies have been only theoretical, since the experimental investigations into the dynamical properties of W(001) have been limited due to technical difficulties. However, this situation is now changing rapidly, with advances in experimental techniques such as electron-energy-loss spectroscopy[15,16] and helium atom scattering.[13,17] It has recently become possible to measure surface phonons in great detail for wave vectors throughout the surface Brillouin zone.

In order to study the dynamical properties and the high-temperature structure of W(001), Ernst, Hulpke, and Toennies[13] have carried out high-resolution helium-atom diffraction and time-of-flight (TOF) energy-loss measurements on clean W(001) along the $\langle 110\rangle(\bar{\Gamma}\bar{M})$ direction, at several temperatures between 220 and 450 K. Their diffraction data suggest that the W(001) surface is ordered and bulklike at high temperatures, and that the transition to $(\sqrt{2}\times\sqrt{2})R45°$ at low temperatures proceeds via an incommensurate phase. The TOF energy-loss spectra in these experiments are obtained at 450 and 280 K. At both temperatures, two surface modes are observed ($A$ and $R$ in Fig. 1), one of which ($A$) shows an anomalous behavior. Ernst *et al.*[13] have interpreted these modes on the basis of the calculations of Wang and Weber[10] and Black, Campbell, and Wallis,[11] suggesting that $A$ is longitudinal and $R$ is the Rayleigh mode.

With the availability of the TOF data of Ernst *et al.*,[13] the dynamical models of W(001) can now be tested against experimental results, i.e., these data provide surface-related constraints that a dynamical model must satisfy. Here we construct force-constant models for W(001), which take into account the TOF data via (nonlinear) least-squares fits to $A$ and $R$, in a slab calculation. Bortolani, Franchini, Nizzoli, and Santoro[18] have successfully used force-constant models to account for the (anomalous) surface phonons observed in the bulk bands of Ag(111). Thus we expect that this approach may also be applicable to the dynamics of W(001). In fact, we will find that the models thus obtained enable us to determine the nature of the $A$ and $R$ modes, and the interactions responsible for the anomalous behavior of $A$. A comparison of these models will also give us information about the significance of the long-range interactions at the surface.

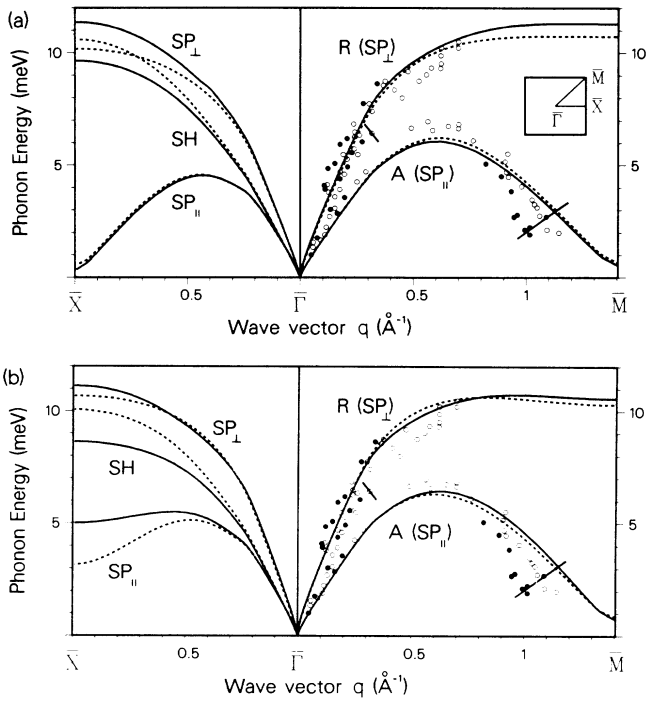


FIG. 1. Dispersion curves in the Rayleigh ($SP_\perp$), longitudinal ($SP_\parallel$), and shear horizontal (SH) modes of unreconstructed W(001), obtained from (a) models 1.1 and 1.2 (solid and dashed curves, respectively), and (b) models 2.1 and 2.2 (solid and dashed curves, respectively). For comparison, the experimental data of Ernst *et al.* (Ref. 13) and the peak width bars are also shown. Open and filled circles denote the data at 450 and 280 K, respectively. Along $\bar{\Gamma}\bar{M}$, the SH mode lies slightly below $A$ and coalesces with $A$ at $\bar{M}$. For this reason, and to let the fit of $A$ with the experimental data be clearly seen, SH is not shown along $\bar{\Gamma}\bar{M}$.

 

The fact that our analysis utilizes experimental surface-phonon data distinguishes it from the previous theoretical investigations of W(001).[8-12]

Our force-constant model for bulk tungsten consists of pairwise central interactions up to third neighbors, and three-body angle-bending interactions. The pairwise interactions yield six force constants $\alpha_i,\beta_i$ $(i=1,2,3)$, where $\alpha_i$ $(\beta_i)$ are radial (tangential) force constants between $i$th neighbors. We consider angle bending interactions associated with the triangles formed by an atom, say $p$, and its two first neighbors, say $i,j$, such that $i,j$ are 2nd neighbors of each other. We associate a stiffness constant $\chi_1$ with the angle at $p$, subtended by $i$ and $j$ (see Ref. 14 for details).

With the use of this model, we first calculate the surface modes of unreconstructed W(001) in an approximation in which only the atoms in the top (surface) layer are assumed to vibrate, while those in the 2nd and subsequent layers remain static. The advantage of this approximation is that it enables us to calculate the surface modes of W(001) *analytically*. These analytical expressions for the dispersion of the surface modes reveal the effect of various force constants on the surface modes, and thus guide us in deciding the free parameters in the subsequent least-squares fits to $A$ and $R$, which involve full slab calculations. These expressions also enable us to show heuristically that $A$ and $R$ must be the longitudinal and the Rayleigh modes, respectively.

The analytical expressions for the dispersion of the Rayleigh $(SP_\perp)$,[19] the longitudinal $(SP_\parallel)$,[19] and the shear horizontal (SH) modes along $\bar{\Gamma}\bar{M}$, to the first order in $\chi_1$ (since $|\chi_1| \ll \alpha_1$), are given by[14]

$$M\omega^2_{SP_\perp}(\bar{q}) = \tfrac{4}{3}(\alpha_1+2\beta_1)+\alpha_2+8\beta_{2s}\sin^2(b\bar{q})+2\alpha_3+2\beta_3+4\beta_{3s}\sin^2(2b\bar{q})+\tfrac{16}{9}\chi_1[5+\cos(2b\bar{q})]\,, \quad (1)$$

$$M\omega^2_{SP_\parallel}(\bar{q}) = \tfrac{4}{3}(\alpha_1+2\beta_1)+\beta_2+4(\alpha_{2s}+\beta_{2s})\sin^2(b\bar{q})+\alpha_3+3\beta_3+4\alpha_{3s}\sin^2(2b\bar{q})+\tfrac{8}{9}\chi_1[8-3\cos(2b\bar{q})]\,, \quad (2)$$

$$M\omega^2_{SH}(\bar{q}) = M\omega^2_{SP_\parallel}(\bar{q})+4(\beta_{3s}-\alpha_{3s})\sin^2(2b\bar{q})\,, \quad (3)$$

where $M$ is the mass of the tungsten atom, $2b$ its bulk lattice constant, $0 \le \bar{q} \le \pi/(2b)$ along $\bar{\Gamma}\bar{M}$, and $\alpha_{is},\beta_{is}$ $(i=2,3)$ the $i$th-neighbor interactions among the surface atoms.

Since a shear horizontal mode cannot be detected by in-plane helium scattering, we need to determine whether $A$ is a longitudinal or a Rayleigh mode. Note that an anomalous behavior along $\bar{\Gamma}\bar{M}$ can arise only because of the $\bar{q}$-dependent terms in Eqs. (1) and (2). Since $\alpha_1,\alpha_2$ are the most significant parameters in our model, it follows that a lowering of $\alpha_{2s}$ in (2) is responsible for the anomalous mode. That is, we conclude that $A$ is longitudinal and that $R$ is the Rayleigh mode.

In order to establish this conclusion rigorously, we consider the full dynamics of the W(001) slab with force constants at its surface as free parameters. We obtain least-squares fits of the calculated surface modes of the slab to the experimental data by varying the free parameters. This is a nonlinear fitting problem and requires iterative calculation of the full slab dynamics. From Eqs. (1) and (2) we see that $\alpha_{2s}$, $\beta_{2s}$, $\alpha_{3s}$, $\alpha_1$, and $\alpha_2$ may be treated as free parameters in the least-squares fits. Note that $\alpha_1$, and $\alpha_2$ in these equations are force constants between the surface atoms and the atoms in the second and third layers, respectively. Hence to be unambiguous, we will henceforth represent them as $\alpha_1'$ and $\alpha_2'$.

For simplicity, we start with a model of bulk tungsten given by Castiel, Dobrzynski, and Spanjaard,[12] which consists of only three independent parameters $\alpha_1$, $\alpha_2$, and $\beta_1(=-\beta_2$, due to the equilibrium condition). We denote it as model 1 and list its parameters in Table I. By considering several combinations of surface force constants as free parameters, we find that variations in $\alpha_{2s},\beta_{2s},\alpha_1'$ or $\alpha_{2s},\beta_{2s},\alpha_2'$ yield the best fits to the data of Ernst *et al.*[13] The values of these parameters which yield the least-squares fits are given in Table II as models 1.1 and 1.2, respectively. Note that the values of $\alpha_{2s}$ and $\beta_{2s}$ are negative and are approximately the same in both models. The dispersions of the longitudinal, shear horizontal, and Rayleigh modes given by these models are shown in Fig. 1(a).

An inspection of Fig. 1(a) shows that the agreement of the Rayleigh mode with the experimental data is quite good. But the peak of $A$ and its falloff for large $\bar{q}$ are not reproduced all that well (although the fit is within the peak widths error bars). To see if this discrepancy is due to the small number of parameters in model 1, we carry out least-squares fits using a six-parameter model (model 2 in Table I), which includes pair interactions up to third neighbors, and the angle bending interaction $\chi_1$ described earlier. Furthermore, in these fits we also let $\alpha_{3s}$ be a free parameter, the reason being that the term $4\alpha_{3s}\sin^2(2b\bar{q})$ in Eq. (2) contributes mostly near the midpoint of $\bar{\Gamma}\bar{M}$ (i.e., near $2b\bar{q}=\pi/2$). Hence this term may be able to "raise" the peak of $A$ without affecting it elsewhere. As before, we find that variations in $\alpha_{3s}$, $\alpha_{2s}$, $\beta_{2s}$, and $\alpha_1'$ or $\alpha_2'$ yield the best fits. The values of these parameters for the least-squares fits are listed in Table II as models 2.1 and

TABLE I. Force constants of bulk tungsten models used in the dynamics of a W(001) slab. All force constants are expressed in $THz^2 M$, where $M$ is the mass of the tungsten atom.

| Model | $\alpha_1$ | $\alpha_2$ | $\alpha_3$ | $\beta_1$ | $\beta_2$ | $\beta_3$ | $\chi_1$ |
|---|---|---|---|---|---|---|---|
| 1 | 6.11 | 4.37 | a | −0.04 | 0.04 | a | a |
| 2 | 5.141 | 3.546 | 0.585 | 0.008 | −0.008 | 0.000 | 0.110 |

[a]Parameter not used in the model.

TABLE II. Force constants in ($THz^2 M$), at the *surface* of a W(001) slab obtained from least-squares fits to the surface-phonon data of Ernst *et al.* (Ref. 13). Models 1.1 and 1.2 are obtained from bulk model 1, and models 2.1 and 2.2 are obtained from bulk model 2.

| Model | $\alpha_{2s}$ | $\beta_{2s}$ | $\alpha_{3s}$ | $\alpha_1'$ | $\alpha_2'$ |
|---|---|---|---|---|---|
| 1.1 | −0.98 | −0.29 | a | 5.00 | b |
| 1.2 | −1.10 | −0.38 | a | b | 2.00 |
| 2.1 | −0.98 | −0.30 | 0.20 | 2.90 | b |
| 2.2 | −1.35 | −0.45 | 0.00 | b | 1.00 |

[a]Parameter not used in the model.
[b]Parameter kept fixed at its bulk value.

2.2, respectively, and the corresponding dispersion curves are shown in Fig. 1(b).

A comparison of Figs. 1(a) and 1(b) shows that even with the six-parameter model with four free parameters in the least-squares fits, the dispersion curves (along $\bar{\Gamma}\bar{M}$) in Fig. 1(b) remain practically unchanged from those in Fig. 1(a). This suggests that the anomaly in $A$ results mainly from the short-range interactions. To verify this explicitly, we independently vary $\alpha_{2s}$, $\beta_{2s}$, $\alpha_1'$, $\alpha_2'$, and find that the falloff of $A$ occurs mainly due to a lowering of $\alpha_{2s}$, and that the falloff becomes steeper as $\alpha_{2s}$ is made more negative. It may therefore seem that with a suitable choice of $\alpha_{2s}$, the falloff may be reproduced very accurately. But if that is done, the W(001) slab exhibits imaginary eigenfrequencies near $\bar{M}$, which is unphysical. This, together with the fact that the values of $\alpha_{2s}$ in all four models of W(001) in Table II are comparable, supports our conclusion that the lowering of $\alpha_{2s}$ is indeed the main mechanism for the occurrence of $A$. Since $\alpha_{2s} \approx -1\ THz^2 M$ is the lowest value of $\alpha_{2s}$ which yields real eigenfrequencies (see Table II), it follows that within a force-constant model the falloff of $A$ cannot be made any steeper than that in Fig. 1. The discrepancy between $A$ and the experimental data may be attributed partly to large errors in the data and partly to the intrinsic limitations of the force-constant models.[20] We do not have a conclusive explanation of the steeper falloff of $A$ at 280 K (filled circles in the figures), since there are not enough data available. However, helium diffraction data of Ernst *et al.*[13] suggest that at 280 K the W(001) surface is not fully $(\sqrt{2}\times\sqrt{2})R45°$ reconstructed, and therefore the 280 K data may be explained the same way as the 450 K data.

With the use of bulk parameters at the W(001) surface, the Rayleigh mode at $\bar{M}$ occurs at ~14 meV. We find that a reduction in $\beta_{2s}$, $\alpha_1'$, or $\alpha_2'$ is required to obtain an agreement of $R$ with the experimental data. This reduction also lowers the longitudinal mode ($A$) to some extent, but the lowering is small and uniform, i.e., it does not yield the observed bell shape of $A$ (which is produced only by changing $\alpha_{2s}$). We find that a reduction in $\beta_{2s}$ and $\alpha_1'$, or that in $\beta_{2s}$ and $\alpha_2'$, yields the best fit to $R$, with a minimum lowering of the peak of $A$.

From Fig. (1) we see that all four models of W(001) agree quite well with the experimental data, and therefore are equally acceptable on the basis of these data. But on physical grounds, 1.1 and 2.1 may be preferable to 1.2 and 2.2, since in 1.1 and 2.1 the force constant $\alpha_1'$ (with second-layer atoms) is modified, whereas in 1.2 and 2.2, $\alpha_2'$ (with third-layer atoms) is modified. In order to choose between the three- and six-parameter models, we need to compare their surface phonons along $\bar{\Gamma}\bar{X}$ (see Fig. 1): The longitudinal mode in the three-parameter models shows an anomaly similar to that along $\bar{\Gamma}\bar{M}$, whereas that in the six-parameter models does not. Although the exact form of the longitudinal-mode dispersion curve in the six-parameter model may depend on the specific model, the above conclusion remains qualitatively valid. Thus, measurements of surface phonons along $\bar{\Gamma}\bar{X}$ should be able to distinguish between these models.

In conclusion, a comparison of the three- and six-parameters models shows that the surface phonons along $\bar{\Gamma}\bar{M}$ are affected mainly by the short-range interactions. However, along $\bar{\Gamma}\bar{X}$ the predictions of these models are substantially different. Thus our analysis shows that surface-phonon measurements along $\bar{\Gamma}\bar{X}$ may provide additional information about the nature of interactions at the W(001) surface—an issue on which there is still no agreement.[8–10]

We are thankful to H. Ernst, E. Hulpke, and J. Toennies for sending us their experimental results prior to publication. This research was supported by the National Science Foundation through Grant No. DMR-8505747 and by the Robert A. Welch Foundation through Grant No. F-433.

*Permanent address: Institut für Theoretische Physik, Universität Regensburg, D-8400 Regensburg, Federal Republic of Germany.

[1]J. E. Inglesfield, Prog. Surf. Sci. **20**, 105 (1985); D. A. King, Phys. Scr. **4**, 34 (1983).
[2]R. A. Barker and P. J. Estrup, J. Chem. Phys. **74**, 1442 (1981).
[3]M. K. Debe and D. A. King, Surf. Sci. **81**, 193 (1979); J. Phys. C **15**, 2257 (1982).
[4]J. A. Walker, M. K. Debe, and D. A. King, Surf. Sci. **104**, 405 (1981).
[5]M. K. Debe and D. A. King, Phys. Rev. Lett. **39**, 708 (1977); J. Phys. C **10**, L303 (1977).
[6]T. E. Felter, R. A. Barker, and P. J. Estrup, Phys. Rev. Lett. **38**, 1138 (1977).
[7]A. J. Melmed and W. R. Graham, Appl. Surf. Sci. **11/12**, 470 (1982).
[8]A. Fasolino, G. Santoro, and E. Tossati, Phys. Rev. Lett. **44**, 1684 (1980); Surf. Sci. **125**, 317 (1983).
[9]L. D. Roelofs and J. F. Wendelken, Phys. Rev. B **34**, 3319 (1986).
[10]X. W. Wang and W. Weber, Phys. Rev. Lett. **58**, 1452 (1987).
[11]J. E. Black, D. A. Campbell, and R. F. Wallis, Surf. Sci. **115**, 161 (1982).
[12]D. Castiel, L. Dobrzynski, and D. Spanjaard, Surf. Sci. **59**, 252 (1976).
[13]H.-J. Ernst, E. Hulpke, and J. P. Toennies, Phys. Rev. Lett. **58**, 1941 (1987).

[14]A. D. Kulkarni and F. W. de Wette, Surf. Sci. **186**, 469 (1987).

[15]J. P. Woods, A. D. Kulkarni, J. L. Erskine, and F. W. de Wette, this issue, Phys. Rev. B **36**, 5848 (1987); J. P. Woods and J. L. Erskine, Phys. Rev. Lett. **55**, 2595 (1985).

[16]H. Ibach and T. S. Rahman, in *Chemistry and Physics of Solid Surfaces,* edited by R. Vanselow and R. Howe (Springer-Verlag, New York, 1984); H. Ibach and D. L. Mills, *Electron Energy Loss Spectroscopy and Surface Vibrations* (Academic, New York, 1982).

[17]J. P. Toennies, J. Vac. Sci. Technol. A **2**, 1055 (1984).

[18]V. Bortolani, A. Franchini, F. Nizzoli, and G. Santoro, Phys. Rev. Lett. **52**, 429 (1984).

[19]SP denotes the *sagittal plane* spanned by the phonon wave vector $\bar{q}$ and the normal to the surface. $SP_{\parallel}$ ($SP_{\perp}$) denotes the surface-phonon polarization, predominantly parallel (perpendicular) to the surface and within the sagittal plane.

[20]It may be possible to reduce this discrepancy by including additional physical parameters such as charge fluctuations.